Available online at www.sciencedirect.com
SCIENCE DIRECT®
Journal of Organometallic Chemistry 691 (2006) 323–330
Journal of Organometallic Chemistry
www.elsevier.com/locate/jorganchem

Ferrocenyl D–π–A conjugated polyenes with 3-dicyanomethylidene-1-indanone and 1,3-bis(dicyanomethylidene)indane acceptor groups: Synthesis, linear and second-order nonlinear optical properties and electrochemistry

Izabela Janowska [a], Janusz Zakrzewski [a,*], Keitaro Nakatani [*,b], Marcin Palusiak [c], Marcin Walak [d], Henryk Scholl [d]

[a] *Department of Organic Chemistry, University of Łódź, 90-136, Łódź, Narutowicza 68, Poland*
[b] *Laboratoire de photophysique et, Photochimie supramoleculaire et, Macromoleculaire (PPSM, CNRS UMR 8531), Ecole Normale Superieure de, Cachan, 61, Avenue du President Wilson, 94235 Cachan Cedex, France*
[c] *Department of Crystallography, University of Łódź, 90-236 Łódź, Pomorska 149/153, Poland*
[d] *Department of General and Inorganic Chemistry, University of Łódź, 90-136 Łódź, Narutowicza 68, Poland*

Received 21 April 2005; received in revised form 18 August 2005; accepted 24 August 2005
Available online 17 October 2005

Abstract

Second-order nonlinear optical chromophores incorporating the ferrocenyl group as an electron donor and 3-dicyanomethylidene-1-indanone and 1,3-bis(dicyanomethylidene)indane acceptor groups, connected by a conjugated polyenic bridge of varied length (**2**[***n***] and **3**[***n***], respectively) have been synthesized. The electronic absorption spectra of these compounds display in the visible region bands attributable to π–π* and metal-to ligand charge transfer (MLCT) transitions. The energies of these transitions are close to those reported earlier for ferrocenyl D–π–A chromophores with the strongest acceptor groups, e.g., with the 3-dicyanomethylidene-2,3-dihydrobenzothiophene-1,1-dioxide group (**1**[***n***]) [V. Alain, M. Blanchard-Desce, C.-T. Chen, S.R. Marder, A. Fort, M. Barzoukas, Synt. Met. 81 (1996) 133]. The solid-state structure of **2**[**3**], determined by X-ray diffraction shows a significant reduction of the bond length alternation (BLA), 0.05 Å, suggesting high first hyperpolarizability. However, a centrosymmetrical packing of molecules of this compound in the crystal excludes its second harmonic generation ability. The $\mu\beta$ values of **2**[***n***] and **3**[***n***], determined by the EFISH technique at 1907 nm are high and increase with the increasing length of the conjugated π-bridge. The highest value of $\mu\beta$ (8720×10^{-48} esu) was determined for **3**[**4**], which is close to that reported for **1**[**4**] ($11\,200 \times 10^{-48}$ esu), the highest value found for a ferrocenyl D–π–A chromophore until now.

Keywords: Ferrocene; 3-Dicyanomethylidene-1-indanone and 1,3-bis(dicyanomethylidene)indane; NLO-chromophore; EFISH; X-ray structure; Electronic absorption spectra; Cyclic voltammetry

1. Introduction

"Push–pull" compounds containing ferrocenyl (Fc) donor group bound to a conjugated polyenic chain capped by an acceptor moiety A, (Fc–π–A), have attracted considerable interest as second-order nonlinear optical (NLO) chromophores [1–15]. They display large first hyperpolarizabilities (β), and some of them second harmonic generation (SHG) ability in the solid state. Although the NLO activity of Fc–π–A molecules usually does not exceed that of their organic counterparts having *p*-aminophenyl or *p*-methoxyphenyl groups in place of the Fc group, they offer an unique possibility of switching of the NLO properties by

* Corresponding author. Tel.: +4842 678 4731; fax: +4842 678 6583.
E-mail address: janzak@uni.lodz.pl (J. Zakrzewski).

0022-328X/$ - see front matter © 2005 Elsevier B.V. All rights reserved.
doi:10.1016/j.jorganchem.2005.08.033

reversible oxidation/reduction of the Fc group [16–18]. Another advantage of Fc–π–A compounds is that introduction of the second substituent (different from the first one) into the substituted Cp ring makes their molecules planary chiral and opens an entry to noncentrosymmetric crystalline materials displaying SHG ability [1,8].

Blanchard-Desce et al. [9,10] have prepared a series of conjugated ferrocenyl polyenes having at the second cap of the conjugated system of varied length potent acceptor units in order to achieve large quadratic nonlinearities. They have found that 3-dicyanomethylidene-2,3-dihydrobenzothiophene-1,1-dioxide moiety endows molecules **1** (Fig. 1) with particularly high values of $\mu\beta$ (the vectorial projection of the hyperpolarizability along the molecular dipole moment direction, a figure of merit for the NLO behaviour of materials rendered noncentrosymmetric by poling chromophores in a polymer matrix) measured by the electric field induced second harmonic (EFISH) generation technique.

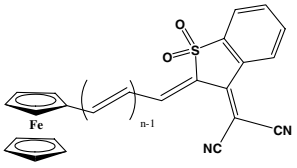

1[*n*]

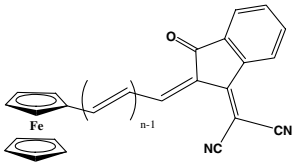

2[*n*]

1[1] μβ(2ω) =160 x 10^{-48} esu
1[2] μβ(2ω) =1400 x 10^{-48} esu
1[3] μβ(2ω) =3000 x 10^{-48} esu
1[4] μβ(2ω) =11200 x 10^{-48} esu

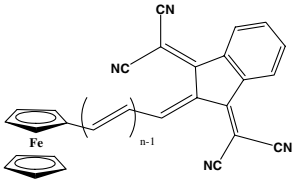

3[*n*]

We have recently synthesized and studied linear and second-order NLO properties of molecules composed of the ferrocenyl and 3-dicyanomethylidene-1-indanone and 1,3-bis(dicyanomethylidene)indane acceptor group linked by one sp^2 carbon, **2**[**1**], and **3**[**1**], respectively [19]. These indanone-based potent electron-acceptor groups were earlier introduced to purely organic molecules and endowed them with particularly large second-order NLO activities [20–23]. We have determined $\mu\beta(2\omega)$ values of **2**[**1**] and **3**[**1**] using the EFISH technique at 1907 nm equal 160×10^{-48} and 280×10^{-48} esu, respectively. These large values, comparable or larger than that of **1**[**1**] suggested us that elongation of the conjugated sp^2 chain between the ferrocenyl and 3-dicyanomethylidene-1-indanone and 1,3-bis(dicyanomethylidene)indane groups may result in compounds displaying giant second-order optical nonlinearities. Herein, we report on synthesis of compounds **2**[**2**]–**2**[**4**] and **3**[**2**]–**3**[**4**], their electronic absorption spectra and EFISH data and their Fe(II)/Fe(III) oxidation potentials measured by cyclic voltammetry.

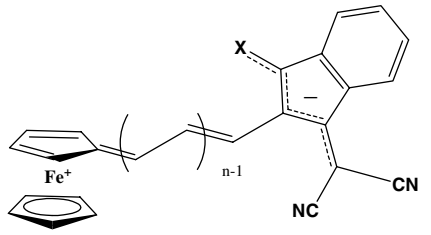

Fig. 1. Charge-separated resonance form of compounds **2**[*n*] and **3**[*n*]. X = O or $C(CN)_2$.

2. Results and discussion

2.1. Synthesis and structure of 2[n] and 3[n]

Compounds **2**[**2**]–**2**[**4**] and **3**[**2**]–**3**[**4**] were prepared from the corresponding ω-ferrocenyl-polyenals **4**[**2**]–**4**[**4**] [24] via Knoevenagel reaction with 3-dicyanomethylidene-1-indanone and 1,3-bis(dicyanomethylidene)indane, respectively (Scheme 1).

Reactions of **4**[**2**]–**4**[**4**] with 3-(dicyanomethylidene)-1-indanone were performed by refluxing of both components in methanol (no basic catalysts is required). Under the same conditions reactions of **4**[**2**]–**4**[**4**] with 1,3-bis(dicyanomethylidene)indane led to complex, intractable mixtures. However, it has been found that this reaction proceeds cleanly in acetic anhydride at 55–60 °C to give **4**[*n*]. The isolated yields of **2**[*n*] and **3**[*n*] were 67–94%. The *all-trans* configuration of the conjugated polyenic chain was confirmed by large values of vicinal coupling constants between protons attached to the same ethylenic bond in the ^{1}H NMR spectra of these compounds (Table 1). Formally, the expected values of coupling constant between *trans* protons in the CH=CH and CH–CH groups

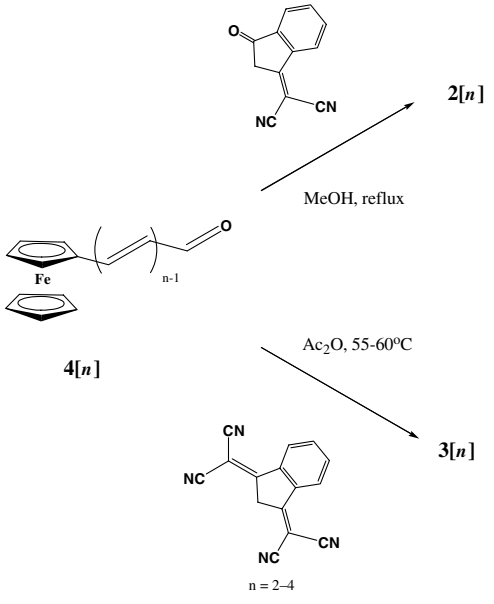

Scheme 1.

Table 1
Coupling constants between vicinal protons along the polyenic chain, numbered from the ferrocenyl end to the acceptor end, in compounds **2**[***n***] and **3**[***n***]

Compound	J_{12} (Hz)	J_{23} (Hz)	J_{34} (Hz)	J_{45} (Hz)	J_{56} (Hz)	J_{67} (Hz)
2[**2**]	13.9	12.0				
2[**3**]	14.8	11.5	13.9	12.0		
2[**4**]	nd	nd	13.9	11.5	13.8	12.0
3[**2**]	14.3	12.2				
3[**3**]	14.5	12.0	13.5	12.5		
3[**4**]	15.5	12.0	14.5	11.6	13.5	12.8

nd, non-determined.

are 16.5 Hz and ~10 Hz, respectively, and the values observed in **2**[***n***] and **3**[***n***] indicate a reduced bond-order alternation [25,26] due to a contribution of the charge-separated limiting resonance form shown in Fig. 1.

Due to such reduced bond-order alternation typical values of vicinal coupling constants for *all-trans* push–pull polyenes are 13.7–16.4 Hz for C–C bonds with dominant double bond character and 9.7–12.0 Hz for C–C bonds with dominant single bond character [25,26].

The values of coupling constants presented in Table 1 (obtained in selective decoupling experiments if necessary) indicate that compounds **2**[***n***] and **3**[***n***] show reduced bond order alternation along the polyenic chain comparable with that reported for for those reported for push–pull polyenes with the strongest D/A strength combination [25,26]. This means that both 3-dicyanomethylidene-1-indanone and 1,3-bis(dicyanomethylidene)indane groups placed at the end of a ferrocenyl polyenic chain behave as very strong electron acceptors.

2.2. Linear and nonlinear optical properties of *2[n] and 3[n]*

Similarly as other ferrocenyl push–pull chromophores, compounds **2**[***n***] and **3**[***n***] display two intense absorption bands in the visible region of their electronic absorption spectra (Table 2). The nature of these transitions and their contributions to NLO properties can be explained by using a number of models [7,27–29], among which the model developed by Barlow et al. [7] is the most generally accepted. According to this model the lower energy band is assigned to a metal-to-acceptor transition, whereas the higher energy band to a transition from the ligand π orbital (HOMO − 3) to the acceptor-based LUMO orbital. Since both transitions have intramolecular charge transfer (ICT) nature and are associated with a considerable increase of molecular dipole moments, strong positive solvatochromic effect (i.e., red-shift with the increasing solvent polarity) is observed. As a rule, transitions displayed by compounds **3**[***n***] are lower in energy than their counterparts for compounds **2**[***n***] (although some exception from this trend are observed, e.g., the lower energy transitions of **3**[**2**] and **2**[**2**] appear in chloroform at the same wavelength, 675 nm). This phenomenon is not completely unexpected since it has been reported that in organic push–pull molecules containing 1,3-indandione acceptor group the replacement of one carbonyl oxygen by the $C(CN)_2$ moiety gives rise to a bathochromic shift of ICT transitions [23]. Consequently, a bathochromic shift is expected to be associated with the similar replacement of the carbonyl oxygen in the 3-dicyanomethylidene-1-indanone group. The observed shift suggests a higher electron acceptor ability of the 1,3-bis(dicyanomethylidene)indane group in comparison to the the 3-dicyanomethylidene-1-indanone group giving rise to a lowering of energy of the acceptor-based orbitals. It was of interest to compare linear optical properties of **2**[***n***] and **3**[***n***] with those reported for **1**[***n***] [10]. Unfortunately, the spectra of the latter compounds were measured in dichloromethane, making strict comparison with our data impossible. Nevertheless, we should emphasize a close similarity between the spectra of **3**[***n***] in chloroform and those of **1**[***n***] in dichloromethane. This similarity indicates very high acceptor ability of the 1,3-bis(dicyanomethylidene)indane acceptor group.

Table 2
Absorption maxima in the visible region of **2**[***n***] and **3**[***n***] in various solvents (for comparison data for **1**[***n***])

Compound	λ_{max}/nm ($\varepsilon_{max} \times 10^{-4}$/cm^{-1} M^{-1})		
	Hexane	Benzene	Chloroform
2[**1**]	408 (0.8)	410 (0.8)	414 (1.0)
	613 (0.4)	622 (0.4)	632 (0.5)
2[**2**]	445 (1.7)	445 (1.4)	446 (1.7)
	637 (1.0)	659 (0.9)	675 (1.0)
2[**3**]	474 (3.2)	487 (3.1)	493 (3.3)
	643 (2.2)	672 (2.2)	690 (2.2)
2[**4**]	501 (2.5)	512 (2.8)	522 (3.9)
	644 (2.0)	600 (2.4)	692 (3.2)
3[**1**]	408 (1.2)	410 (1.2)	414 (1.2)
	637 (0.7)	656 (0.7)	659 (0.5)
3[**2**]	463 (1.9)	468 (1.8)	472 (1.8)
	637 (1.0)	659 (0.9)	675 (1.0)
3[**3**]	493 (4.2)	508 (4.2)	513 (4.0)
	692 (3.2)	716 (3.2)	733 (3.5)
3[**4**]	518 (2.2)	533 (2.3)	547 (2.4)
	696 (2.0)	717 (2.2)	745 (2.2)
1[**1**]			419 (1.3)[a]
			667 (0.7)[a]
1[**2**]			475 (1.7)[a]
			721 (0.7)[a]
1[**3**]			517 (4.8)[a]
			746 (3.3)[a]
1[**4**]			552 (2.9)[a]
			743 (2.3)[a]

[a] Values taken from [10] (solvent: dichloromethane).

2.3. Solid-state structure of *2[3]*

The solid-state structure of **2**[**3**] has been determined by the X-ray diffraction method. The crystal data are collected in Table 3 and selected bond lengths and angles in Table 4. The ORTEP drawing of this compound is shown in Fig. 2.

The distances between the iron atom and the planes of the substituted and unsubstituted cyclopentadienyl ligand

are 1.6392(8) and 1.6544(8) Å, respectively. The planes of these ligands are not parallel and form an angle of 2.4(3)°. The methine carbon C6 is tilted from the substituted Cp plane towards iron and the angle between the C1A–C6 bond and this plane is 1.7(3)°. The distance between iron and C6 is 3.078(5) Å. The polyenic chain exhibits nearly planar zigzag "all-*E*" conformation and reduced bond length alternation (BLA, defined as the average difference between C=C and C–C bond lengths) equals −0.05 Å. As observed earlier in structures of push–pull polyenes, the BLA is more pronounced near to the donor (ferrocenyl) end than near to the acceptor length. The plane of the polyenic chain forms with the plane of the substituted Cp ligand an angle of 13.1(3)° and with the plane of the five-membered ring in the indanone moiety an angle of 8.7(3)°. The angle between the above-mentioned five-membered ring planes is 22.9(2)°.The atoms of the dicyanomethylidene moiety do not significantly deviate from the indane ring plane, the maximum deviation being 0.365(6) Å for N2 and the carbonyl oxygen O1 lies in this

Table 3
Crystal data and structure refinement details for **2**[**3**]

Empirical formula	$C_{27}H_{18}FeN_2O$
Formula weight	422.28
Crystal description	Green plate
Crystal size (mm^3)	$0.5 \times 0.17 \times 0.05$
Space group	$P2_1/c$
Unit cell dimensions	
a (Å)	9.8905(18)
b (Å)	7.4650(19)
c (Å)	28.3448(19)
β (°)	94.047(11)
V (Å^3)	2087.6(7)
D_{calc} (g cm^{-3})	1.407
Data collection	
Diffractometer	Rigaku AFC5S
Radiation type λ (Å)	Cu Kα 1.54178
μ (mm^{-1})	5.957
T (K)	293(2)
Data collected (h,k,l)	$-8 \leqslant h \leqslant 11$, $-7 \leqslant k \leqslant 8$, $-33 \leqslant l \leqslant 33$
Numbers of reflections measured	3866
Numbers of independent reflections	3643
R_{int}	0.0423
Numbers of reflections with $I > 2\sigma(I)$	1706
Solution and refinement	
Solution	Direct methods
Refinement method	Full-matrix least-squares on F^2
Number of parameters	280
$R(F)$[a]	0.1459
$wR(F^2)$[b]	0.1396[c]
$R(F)$[a]	0.0533 for 1706 reflections[c]
$wR(F^2)$[b]	0.1250 for 1706 reflections[c]
$(\Delta/)_{max}$	0.000
Different peak/hole (e Å^{-3})	0.707/−0.45

[a] $R(F) = \sum(|F_o - F_c|)/|F_o|$.
[b] $wR(F^2)=[\sum w(|F_o - F_c|)^2/\sum|F_o|^2]^{1/2}$.
[c] $w = \exp[(3 \sin\theta)^2]/[\sigma^2(F_o^2) + (0.0636P)^2]$ where $P = 0.33333F_o^2 + 0.66667F_c^2$.

Table 4
Selected geometric parameters for **2**[**3**] [Å, °]

Fe–C1A	2.036(5)
Fe–C2A	2.036(5)
Fe–C3A	2.038(5)
Fe–C4A	2.046(5)
Fe–C5A	2.018(5)
Fe–C1B	2.045(6)
Fe–C2B	2.027(6)
Fe–C3B	2.034(6)
Fe–C4B	2.023(6)
Fe–C5B	2.049(7)
C1A–C6	1.425(6)
C6–C7	1.359(7)
C10–C11	1.376(7)
C12–C20	1.360(7)
C20–C21	1.440(8)
C20–C22	1.435(7)
C21–N1	1.150(8)
C22–N2	1.121(7)
C15–O1	1.201(6)
C12–C20–C21	123.4(5)
C12–C20–C22	125.4(4)
C12–C11–C10	128.6(4)
C15-C11–C10	123.5(5)
C5A-C1A–C6	125.3(4)
C2A–C1A–C6	128.7(4)
C13–C12–C11–C10	−178.4(5)
C13–C12–C11–C15	−1.7(5)
C13–C12–C20–C21	−178.6(5)
C13–C12–C20–C22	6.2(8)
C2A–C1A–C6–C7	13.7(9)
C6A–C1A–Fe–C1B	0.9(5)

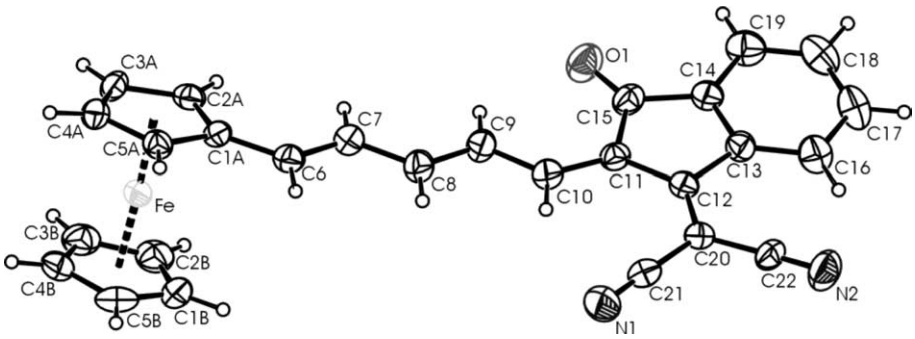

Fig. 2. The ORTEP drawing of the molecule of **2**[**3**] with atom numbering scheme. Displacement ellipsoids are drawn at 40% probability level.

plane. Interestingly, the structure of **2**[**3**] shows intramolecular hydrogen bonds between C9–H9 and O1, C10–H10 and cyano group C21≡N1, and C16–H16 and C22≡N2. In the case of the last two bonds it proved impossible to distinguish between hydrogen bonds with the π-systems of the cyano groups or with the relevant nitrogen atoms (N1 and N2). Hence, in Table 5, presenting geometries of these bonds, the relevant distances and angles were calculated assuming that N1 and N2 are proton acceptors. It is worthy noting that analogous hydrogen bonds were not observed in the structures of **2**[**1**] and **3**[**1**].

The molecular packing of is shown in Fig. 3. It exhibits antiparallel "head-to tail" arrangement of molecules in the centrosymmetrical space $P2_1/c$ group. This spatial arrangement excludes bulk second-order NLO properties for this compound.

The above data clearly indicate significant interactions of the donor (ferrocenyl) and acceptor (dicyanomethylideneindanone) group across the polyenic chain. Unsurprisingly, this interactions in **2**[**3**] seems to be weaker than those detected in compounds with a shorter π-bridge (**2**[**1**] or **3**[**1**]). This can be deduced from weaker deformations of the ferrocenyl unit towards η^6-fulvenic structure characteristic for the charge-separated form. For comparison, the angle between the Cp ring planes in **2**[**1**] is 4.0(2)°, the tilting angle of the C1A–C6 bond 10.2(3)°, and the distance C6–Fe, 2.954(4) Å [19].

Table 5
Hydrogen-bonding geometry (Å, °) for **2**[**3**]

D–H···A	D–H	H···A	D···A	D–H···A
C(9)–H(9)···O(1)	0.93	2.36	2.965(7)	123(1)
C(10)–H(10)···N(1)	0.93	2.59	3.448(7)	154(1)
C(16)–H(16)···N(2)	0.93	2.60	3.385(8)	143(1)

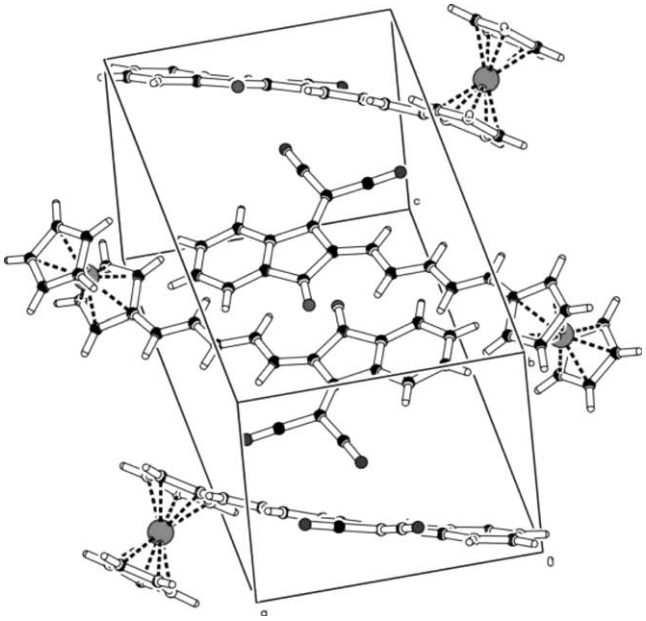

Fig. 3. View of the molecular packing in the unit cell of **2**[**3**].

From the standpoint, the value of BLA calculated for **2**[**3**] should correspond to the maximal absolute value of β. However, it should be kept in mind that the solid state provides polar environment favoring charge separation, and in solution in a nonpolar or weakly polar solvent the BLA may be higher, resulting in a smaller value of β.

2.4. Second-order nonlinear optical properties of *2[n]* and *3[n]*

The second-order nonlinear optical properties of **2**[***n***] and **3**[***n***] were determined using the EFISH technique at $\lambda = 1907$ nm. The values of $\mu\beta(2\omega)$ are gathered in Table 6. We have not calculated frequency-independent (static) values $\mu\beta(0)$ because the two-level model usually used in calculations is not applicable for ferrocenyl compounds (more than one electronic transition contribute to β) [7]. As is seen from Table 6 the values of $\mu\beta(2\omega)$ of **2**[***n***] and **3**[***n***] increase with the increasing length of the conjugated polyenic linker. As observed for similar D–π–A systems [10,14,30] this increase follows a power law ($\mu\beta \sim n^k$) with the exponent k equals 2.5 and 2.3 for **2**[***n***] and **3**[***n***], respectively. These values are lower than that reported for compounds **1**[***n***] (2.9) [10], which leads to lower values of $\mu\beta$ of higher members of series **2**[***n***] and **3**[***n***] in comparison to those of **1**[***n***]. Nevertheless, it should be noted that values of $\mu\beta$ of compounds **2**[**4**] and **3**[**4**], 3900×10^{-48} and 8720×10^{-48} esu, respectively, are among the highest values of this parameter reported for ferrocenyl compounds to date. To our knowledge, comparable values of $\mu\beta(2\omega)$ (up to $5000 \pm 1500 \times 10^{-48}$ esu) were found only for ferrocenyl compounds having polynitrofluorene acceptor groups [11]. Compounds having weaker acceptor groups (e.g., formyl, dicyanomethylidene) exhibit significantly weaker $\mu\beta(2\omega)$ values even when they bear long polyenic chain [6,31].

Table 6
EFISH data for compounds **1**[***n***]–**3**[***n***] determined at 1907 nm in chloroform

Compound	$\mu\beta(2\omega)$ (10^{-48} esu)[a]
2[**1**]	140[b]
2[**2**]	650
2[**3**]	2600
2[**4**]	3900
3[**1**]	280[b]
3[**2**]	1080
3[**3**]	2090
3[**4**]	5200 (8720)[d]
1[**1**]	160[c]
1[**2**]	1400[c]
1[**3**]	3000[c]
1[**4**]	11 200[c]

[a] The error in the measurements is estimated to be ±20%.
[b] Values taken from [19].
[c] Values taken from [10].
[d] Value extrapolated to the infinite dilution.

Table 7
Cyclic voltammetric data for compounds **2**[*n*] and **3**[*n*]

Compound	$E_{1/2}$/mV vs. (Fc^+/Fc)	ΔE_p/mV[a]	D_{ox}/cm^2 s^{-1}[b]	D_{red}/cm^2 s^{-1}[b]	$k_s \times 10^{-2}$/cm s^{-1}[c]
2[**1**][a]	292	77	1.67×10^{-8}	1.18×10^{-8}	1.99
2[**2**]	177	94	1.45×10^{-6}	3.61×10^{-6}	0.24
2[**3**]	108	92	8.21×10^{-6}	7.28×10^{-6}	0.41
2[**4**]	99	209	6.37×10^{-7}	7.15×10^{-7}	0.11
3[**1**][a]	318	88	2.62×10^{-4}	2.43×10^{-4}	0.60
3[**2**]	178	91	1.08×10^{-5}	1.19×10^{-5}	0.52
3[**3**]	121	97	1.40×10^{-5}	1.42×10^{-5}	0.55
3[**4**]	66	96	1.02×10^{-5}	1.02×10^{-5}	0.50

[a] Values taken from [19].
[b] Diffusion coefficient.
[c] Standard rate constant.

2.5. Redox properties

The redox properties of the synthesized compounds were studied by cyclic voltammetry in acetonitrile solutions and the relevant data are gathered in Table 7. A quasi-reversible, monoelectronic ($\Delta E_p < 100$ mV) redox process was observed for **2[1]**–**2**[**3**] and **3**[*n*], corresponding to the transformation of the ferrocene unit to the ferrocenium species. Compound **2**[**4**] showed larger value of ΔE_p (209 mV), suggesting stronger irreversibility and/or slower electron transfer. It may result from reorientation of the molecule on the electrolyte/working electrode interface.

In comparison to ferrocene, the oxidation potentials of all investigated compounds are shifted anodically, due to the electron-withdrawing nature of 3-dicyanomethylidene-1-indanone and 1,3-bis(dicyanomethylidene)indane end groups. The similar, high values of the Fe^{II}/Fe^{III} redox potential were reported for compounds **1**[**1**]–**1**[**3**] (325, 200 and 100 mV in CH_2Cl_2, respectively) [7]. These values reveal efficient electron withdrawal from the ferrocenyl group even across relatively long linker. In contrast, linkers containing aromatic rings usually give rise to lower Fe^{II}/Fe^{III} redox potentials (<60 mV), due to unfavorable loss of aromacity in the zwitterionic, charge-separated resonance structures [13]. As expected, Fe^{II}/Fe^{III} redox potentials decrease with the increasing length of the polyenic bridge. Unexpectedly, there is no simple relationship between oxidation potentials of **2**[*n*] and **3**[*n*]. For $n = 1, 3$ the oxidation potentials of compounds **3**[*n*] are higher than those of **2**[*n*], whereas a reverse effect is observed for $n = 2, 4$.

3. Conclusion

We have shown that compounds **2**[*n*] and **3**[*n*], bearing 3-dicyanomethylidene-1-indanone and 1,3-bis(dicyanomethylidene)indane groups at the end of the ferrocenyl polyenic chain have a push–pull character and display very large values $\mu\beta(2\omega)$ measured by the EFISH technique. They are therefore promising chromophores for electrically poled polymer NLO systems.

4. Experimental

All syntheses were performed under an atmosphere of dry pure argon. Solvents were freshly distilled over the appropriate drying agents immediately prior to use. Polyenals **4**[**2**]–**4**[**4**] were prepared according to the literature method [24]. All other reagents were commercially available (Fluka, Aldrich) and were used as received. Chromatographic separations were carried out on Kieselgel 60 (230–400 mesh ASTM) purchased from Merck, using chloroform–hexane (1:1) as eluent. ^{1}H NMR spectra were recorded in $CDCl_3$ solutions on a Varian Gemini 200 BB spectrometer at 200 MHz or a Bruker DRX 500 spectrometer at 500 MHz. Electronic absorption spectra were recorded on a Helios α spectrometer.

4.1. Syntheses of compounds 2[2]–2[4]

To a boiling solution of **4**[*n*] (0.2 mmol) in methanol (5 ml), 3-dicyanomethyleneindan-1-one (110 mg, 0.57 mmol) was added, and the solution was stirred without heating for 15 min. After evaporation of the solvent the product was isolated by chromatography and crystallisation from chloroform–hexane.

Compound **2**[**2**]: Yield: 88%. Brown crystals. δ (^{1}H): 8.68 (m, 1H), 8.38 (m, 2H), 7.89(m, 1H), 7.76 (m, 2H), 7.47 (d, $J = 13.9$ Hz, 1H), 4.78 (m, 4H), 4.26 (m, 5H). IR (KBr,): 2216 cm^{-1} ($\nu_{C\equiv N}$), 1696 cm^{-1} ($\nu_{C=O}$). Anal. Found: C, 71.90; H, 3.94; N, 6.72%. Calc. for $C_{25}H_{16}FeN_2O$: C, 72.12; H, 3.85; N, 6.73.

Compound **2**[**3**]: Yield: 88%. Green crystals. δ (^{1}H): 8.67 (m, 1H), 8.42 (d, $J = 12.0$ Hz, 1H), 8.19 (dd, $J = 13.9$ Hz, 12.0 Hz, 1H), 7.90 (m, 1H), 7.69 (m, 1H), 7.17 (dd, $J = 13.9$ Hz, 11.5 Hz), 7.02 (d, $J = 14.8$ Hz, 1H), 6.78 (d, $J = 11.5$ Hz, 1H), 4.58 (s, 4H), 4.20 (m, 5H). IR (KBr): 2220 ($\nu_{C\equiv N}$), 1697 cm^{-1} ($\nu_{C=O}$). Anal. Found: C, 73.04; H, 4.36; N, 6.14%. Calc. for $C_{27}H_{18}FeN_2O$: C, 73.32; H, 4.10; N, 6.33.

Compound **2**[**4**]: Yield: 90%. Deep green crystals. δ (^{1}H): 8.64 (m, 1H), 8.39 (d, $J = 12.0$ Hz, 1H), 8.25 (dd, $J = 13.9$ Hz, 11.9 Hz, 1H), 7.89(m, 1H), 7.78(m, 2H), 7.16 (dd, $J = 13.8$ Hz, 11.5 Hz, 1H), 6.68 (m, 4H), 4.50 (m,

2H), 4.47 (m, 2H), 4.17 (m, 5H). IR (KBr,): 2226 ($\nu_{C\equiv N}$),1699 cm^{-1} ($\nu_{C=O}$). Anal. Found: C, 71.55; H, 4.21; N, 6.36%. Calc. for $C_{29}H_{20}FeN_2O \times 0.2CHCl_3$: C, 71.25; H, 4.14; N, 5.69.

4.2. Syntheses of compounds 3[2]–3[4]

A solution of **4**[***n***] (0.5 mmol) and 1,3-bis(dicyanomethylidene)indane (80 mg, 0.33 mmol) in acetic anhydride (12 ml) was heated to 55–60 °C for 1.5 h. After evaporation of the solvent the product was isolated by chromatography and crystallisation from chloroform–hexane.

Compound **3**[**2**]: Yield: 63%. Brown crystals. δ (^{1}H): 8.49 (dd, $J = 3.3$ Hz, $J = 5.8$ Hz, 1H), 8.42 (m, 2H), 8.14 (d, $J = 12.2$ Hz, 1H), 7.66 (dd, $J = 3.2$ Hz, $J = 5.8$ Hz, 1H), 7.46 (d, $J = 14.3$ Hz, 1H), 6.79 (dd, $J = 12.2$ Hz, $J = 14.3$ Hz, 1H), 4.81 (t, $J = 1.9$ Hz, 2H), 4.71 (t, $J = 1.9$ Hz, 2H), 4.26 (s, 5H). IR (KBr): 2216 cm^{-1} ($\nu_{C\equiv N}$). Anal. Found: C, 72.31; H, 2.95; N, 11.76%. Calc. for $C_{28}H_{16}FeN_4$: C,72.40; H, 3.37; N, 12.07.

Compound **3**[**3**]: Yield: 85%. Violet-brown crystals. δ (^{1}H): 8.55 (m, 2H), 8.19 (d, $J = 12.5$ Hz, 1H), 7.73 (m, 2H), 7.21 (dd, $J = 13.5$ Hz, $J = 12.0$ Hz, 1H), 7.10 (d, $J = 14.5$ Hz, 1H), 6.77 (dd, $J = 14.5$ Hz, $J = 12.0$ Hz, 1H), 6.73 (dd, $J = 12.5$ Hz, 1H), 4.65 (t, $J = 1.8$ Hz, 2H), 4.60 (t, $J = 1.8$ Hz, 2H), 4.21 (s, 5H). IR (KBr): 2220 cm^{-1} ($\nu_{C\equiv N}$). Anal. Found: C, 73.80; H, 4.07; N, 11.27%. Calc. for $C_{30}H_{18}FeN_4$: C,73.47; H, 3.67; N, 11.43.

Compound **3**[**4**]: Yield: 94%. Violet crystals. δ (^{1}H): 8.55 (dd, $J = 3.1$ Hz, $J = 6.0$ Hz, 1H), 8.18 (d, $J = 12.8$ Hz, 1H), 7.73 (dd, $J = 3.1$ Hz, $J = 6.0$ Hz, 2H), 7.21 (dd, $J = 13.5$ Hz, $J = 11.6$ Hz, 1H), 6.87 (dd, $J = 12.0$ Hz, $J = 14.5$ Hz, 1H), 6.83 (d, $J = 15.5$ Hz, 1H), 6.75 (dd, $J = 13.5$ Hz, $J = 12.8$ Hz, 1H), 6.63 (dd, $J = 14.5$ Hz, $J = 11.6$ Hz, 1H), 6.59 (dd, $J = 12.0$ Hz, $J = 15.5$ Hz, 1H), 4.53 (s, 4H), 4.19 (s, 5H). IR (KBr): 2221 cm^{-1} ($\nu_{C\equiv N}$). Anal. Found: C, 74.63; H, 3,75; N, 10.80%. Calc. for $C_{32}H_{20}FeN_4$: C,74.40; H, 3.91; N, 10.85.

4.3. X-ray crystallographic study

Data were collected on a Rigaku AFC5S diffractometer using Cu Kα ($\lambda = 1.54178$ Å) X-ray source and a graphite monochromator. Analytical absorption corrections was applied. Experimental details are given in Table 3. The crystal structures were solved by direct methods using SHELXS-86 [32] and refined by full-matrix least-square method using SHELXL-97 [33]. All hydrogen atoms except for H2 atom were refined using ridig body model. The molecular geometry was calculated by PARST [34] and PLATON [35].

4.4. EFISH measurements

The principle of the EFISH generation technique is described elsewhere [36,37]. In order to avoid reabsorption of the generated second harmonics the data were recorded using the 1.907 μm, 10 ns incident laser pulses. The compounds were dissolved in chloroform at various concentrations (0–5 mM). The centrosymmetry of the solution was broken by dipolar orientation of the chromophores with a high voltage pulse (around 5 kV applied on 2 mm during 5 μs) synchronised with the laser pulse. The compounds were dissolved in chloroform at various concentrations (0–5 mM) and put into the cell. Calibration of the cell was made by monitoring the second harmonic signal generated by a series of solutions of 2-methyl-4-nitroaniline in chloroform ($\mu\beta = 71 \times 10^{-48}$ esu).

4.5. Cyclic voltammetry

The experiments were carried out using standard three-electrode system with a platinum mesh as an auxiliary electrode and the working polycrystalline gold electrode prepared by means of electrochemical cleaning in 1.0 M $HClO_4$. A classical SCE (in water KCl_{sat} solutions, connected by Luggin capillary and electrolytic bridge with acetonitrile supporting electrolyte) one was used as a reference electrode. All measurements were conducted by means of the PAR 273 potentiostat-galvanostat. The CorWare and CorView 2.4 programs were used for data base (with ± 0.001 V of measured potentials and $\pm 1 \times 10^{-5}$ accuracy). The measurements were carried out in acetonitrile (Fluka AG, *p.a.*) without purification. Tetraethylammonium perchlorate (Et_4NClO_4, 0.1 mol dm^{-3} electrolyte, FLUKA A.G. *p.a.*) was used as a supporting electrolyte. The sweep potential rate was 0.020–0.200 V s^{-1}.

Acknowledgment

Financial support from the Polish-French scientific exchange program (POLONIUM 2005) is gratefully acknowledged.

References

[1] S. Di Bella, Chem. Soc. Rev. 30 (2001) 355.
[2] I.R. Whittal, A.M. McDonagh, M.P. Humphrey, M. Samoc, Adv. Organomet. Chem. 42 (1998) 291.
[3] N.J. Long, Angew. Chem., Int. Ed. Engl. 34 (1995) 21.
[4] D.R. Kanis, M.A. Ratner, T.J. Marks, Chem. Rev. 94 (1994) 195.
[5] J. Heck, S. Dabek, T. Meyer-Friedrichsen, H. Wong, Coord. Chem. Rev. 190–192 (1999) 1217.
[6] Y. Liao, B.E. Eichinger, K.A. Firestone, M. Haller, J. Luo, W. Kaminsky, J.B. Benedict, P.J. Reid, A.K.-Y. Jen, L.R. Dalton, B.H. Robinson, J. Am. Chem. Soc. 127 (2005) 2758.
[7] S. Barlow, H.C. Bunting, C. Ringham, J.C. Green, G.U. Bublitz, S.G. Boxer, J.W. Perry, S.R. Marder, J. Am. Chem. Soc. 121 (1999) 3715.
[8] G. Balavoine, J.-C. Daran, G. Iftime, P.G. Lacroix, E. Manoury, J. Delaire, I. Maltey-Fanton, K. Nakatani, S. Di Bella, Organometallics 18 (1999) 21.
[9] V. Alain, A. Fort, M. Barzuokas, C.-T. Chen, M. Blanchard-Desce, S.R. Marder, J.W. Perry, Inorg. Chim. Acta 242 (1996) 43.
[10] V. Alain, M. Blanchard-Desce, C.-T. Chen, S.R. Marder, A. Fort, M. Barzoukas, Synth. Met. 81 (1996) 133.

[11] A.J. Moore, A. Chesney, M.R. Bryce, A.S. Batsanov, J.F. Kelly, J.A.K. Howard, I.F. Perepichka, D.F. Perepichka, G. Meshulam, G. Berkovic, Z. Kotler, R. Mazor, V. Khodorkovsky, Eur. J. Org. Chem. (2001) 2671.
[12] M. Malaun, R. Kowallick, A.M. McDonagh, M. Marcaccio, R.L. Paul, I. Asselberghs, K. Clays, A. Persoons, B. Bildstein, C. Florini, J.-M. Nunzi, M.D. Ward, J.A. McCleverty, J. Chem. Soc., Dalton Trans. (2001) 3025.
[13] E. Peris, Coord. Chem. Rev. 248 (2004) 279.
[14] K.N. Jayaprakash, P.C. Ray, I. Matsuoka, M.B. Bhadbhade, V.G. Puranik, P.K. Dass, H. Nishihara, A. Sarkar, Organometallics 18 (1999) 3851.
[15] T. Farrell, A.R. Manning, T.C. Murphy, T. Meyer-Friedrichsen, J. Heck, I. Asselberghs, A. Persoons, Eur. J. Inorg. Chem. (2001) 2365.
[16] T. Kondo, S. Horiuchi, I. Yagi, S. Ye, K. Uosaki, J. Am. Chem. Soc. 121 (1999) 391.
[17] I. Asselberghs, K. Clays, A. Persoons, A.M. McDonagh, M.W. Ward, J.A. McCleverty, Chem. Phys. Lett. 368 (2003) 408.
[18] M. Malaun, Z.R. Reeves, R.L. Paul, J.C. Jeffery, J.A. McCleverty, M.D. Ward, I. Asselberghs, K. Clays, A. Persoons, Chem. Commun. (2001) 49.
[19] I. Janowska, J. Zakrzewski, K. Nakatani, J. Delaire, M. Palusiak, M. Walak, H. Scholl, J. Organomet. Chem. 675 (2003) 35–41.
[20] S.-S. Sun, C. Zhang, L.R. Dalton, S.M. Garner, A. Chen, W.H. Steier, Chem. Mater. 8 (1996) 2539.
[21] G. Meshulam, G. Berkovic, Z. Kotler, A. Ben-Asuly, R. Mazor, L. Shapiro, V. Khodorowsky, Synth. Met. 115 (2000) 219.
[22] M. Gonzalez, N. Martin, J.L. Segura, C. Seoane, J. Garin, J. Orduna, R. Alcala, C. Sanchez, B. Villacampa, Tetrahedron Lett. 40 (1999) 8599.
[23] I. Ledoux, J. Zyss, E. Barni, C. Barolo, N. Diulgeroff, P. Quagliotto, G. Viscardi, Synth. Met. 115 (2000) 213–217.
[24] D. Plaźuk, I. Janowska, A. Kłys, A. Hameed Abed Ali, J. Zakrzewski, Synth. Commun. 33 (2003) 381.
[25] M. Blanchard-Desce, V. Alain, P.V. Bedworth, S.R. Marder, A. Fort, C. Runser, M. Barzoukas, S. Lebus, R. Wortmann, Chem. Eur. J. (1997) 1091.
[26] V. Alain, S. Rédoglia, M. Blanchard-Desce, S. Lebus, K. Lukaszuk, R. Wortmann, U. Gubler, C. Bosshard, P. Günter, Chem. Phys. 245 (1999) 51.
[27] D.R. Kanis, M.A. Ratner, T.J. Marks, J. Am. Chem. Soc. 112 (1990) 8203.
[28] J.C. Calabrese, L.T. Cheng, J.C. Green, S.R. Marder, W. Tam, J. Am. Chem. Soc. 113 (1991) 7227.
[29] D.R. Kanis, M.A. Ratner, T.J. Marks, J. Am. Chem. Soc. 114 (1992) 10338.
[30] H. Meier, Angew. Chem. Int. Ed. 44 (2005) 2482.
[31] M. Blanchard-Desce, C. Runser, A. Fort, M. Barzoukas, J.-M. Lehn, V. Bloy, V. Alain, Chem. Phys. 199 (1995) 253.
[32] G.M. Sheldrick, SHELXS-86: Program for Crystal Structure Solution, University of Göttingen, Göttingen, Germany, 1990.
[33] G.M. Sheldrick, SHELXL-97: Program for the Refinement of Crystal Structures, University of Göttingen, Göttingen, Germany, 1997.
[34] M. Nardelli, Comput. Chem. 7 (1983) 95.
[35] A.L. Spek, PLATON and PLUTON: Programs for Molecular Geometry Calculation, University of Utrecht, Utrecht, The Netherlands, 1990.
[36] D.M. Burland, C.A. Walsh, F. Kajzar, C. Sentein, J. Opt. Soc. Am. B (1991) 2269.
[37] I. Maltey, J. Delaire, K. Nakatani, P. Wang, X. Shi, S. Wu, Adv. Mater. Opt. Electron. 6 (1996) 233.